A Study of Charge-Transfer Reactions on (110) Single-Crystal Nickel Surfaces in Nickel Sulfamate Electrolyte Using Electrochemical Impedance Spectroscopy

M. Saitou,* K. Hamaguchi, and K. Inoue

Department of Mechanical Systems Engineering, University of the Ryukyus, 1 Senbaru Nishihara-cho, Okinawa, 903-0213 Japan

Received: July 31, 2002; In Final Form: September 24, 2002

Electrochemical impedance spectroscopy measurements under a small alternating current density were performed to investigate electrochemical reactions on (110) single-crystalline nickel surfaces in nickel sulfamate electrolyte. The reaction impedance shows a power law of the ac modulation frequency, and two exponents for the reaction resistance and reaction capacitance are found to approximately agree with the values predicted by a homogeneous charge-transfer reaction model. In addition, the Nyquist diagrams exhibit the absence of inductive loops for the frequency range from 50 mHz to 100 kHz. A condition for the existence of inductive loops derived in this study suggests that the electrocrystallization of Ni^{2+} ions may take place in the slow reaction step $Ni^{2+} + e^- \rightarrow Ni^+_{abs}$ and in the fast reaction step $Ni^+_{abs} + e^- \rightarrow Ni$.

1. Introduction

Many investigations into kinetic electrode reactions in nickel electrodepositon in Watt's electrolyte, mainly containing $NiSO_4$, $NiCl_2$ and H_3BO_3, have been made using electrochemical impedance spectroscopy (EIS).[1,2] The EIS measurements lead to the conclusion that the electrocrystallization of nickel ions will occur in multistep reactions, which allows us to understand the behaviors of inhibitors and adsorbed intermediates. However, there have been very few reports of the EIS measurements that focus on reaction impedances that scale as $Rr \propto \omega^{-\alpha}$ and $(\omega Cr)^{-1} \propto \omega^{-\beta}$ where Rr is the reaction resistance, Cr is the reaction capacitance, and ω is the ac modulation frequency. The exponents of α and β characterize the charge-transfer reactions. In addition, EIS measurements in nickel sulfamate electrolyte, which has been used for electroforming[3] that requires high speeds of deposition, have not been reported.

EIS enables us to study kinetic electrode reactions through a layer between electrodes and electrolyte. A small alternative current imposed between working and counter electrodes causes a concentration wave that behaves as if electrical components. In general, the electrochemical behaviors of the layer between the working electrode and electrolyte are described by equivalent circuit models[4] comprising electrical components (resistors, capacitors, and inductors) and specialized electrochemical elements (Warburg impedance[5,6] and reaction impedance[7]). An overvoltage caused by the small alternative current fluctuates with a phase shift, which is electrically observed as impedance that is called the reaction impedance. The reaction impedances have been derived from the Fick's diffusion equation for a semi-infinite diffusion.[8,9] According to the theoretical results, the reaction impedance obeys the power law and the exponents of α and β determine whether the electrode reaction is homogeneous or heterogeneous. Information on the type of the charge-transfer reaction is of importance for the studies of nucleation[10] and growth models[11] in electrodeposition. In this paper, we will show that the reaction impedance in nickel sulfamate electrolyte obeys the power law and that the charge-transfer reaction is homogeneous.

The Nyquist diagrams in Watt's electrolyte have been reported, which show the presence of inductive loops for the frequency range from a few to dozens of hertz. The faradaic impedance analysis assumed the presence of adsorbed intermediate ions[2,12] and makes it clear that the Nyquist diagram may have an inductive loop in some cases.[13] Thus, the presence of the inductive loops suggests that the electrocrystallization of nickel ions takes place in many successive steps, for example, two successive faradic reactions[2,12] of adsorbed nickel ions Ni^+_{ads} such as $Ni^{2+} + e^- \rightarrow Ni^+_{ads}$ and $Ni^+_{ads} + e^- \rightarrow Ni$. In this paper, we will report that the EIS measurements in nickel sulfamate show the absence of inductive loops in the Nyquist plots that are different from the results in Watt's electrolyte, and discuss a possibility of the multistep reactions in view of a condition necessary for the EIS measurement to have an inductive loop using a linear perturbation theory and equivalent circuit model.[4]

The surfaces with fractal dimensions[14] and grain-boundaries[15] are known to affect the faradic impedance. For example, the effect of grain-boundaries may be considered to give inhomogeneous reaction rates due to differences of activation energies. In this study, single-crystalline nickel disks of high-purity, 5N were prepared to avoid these effects. These disks were polished to appear mirrorlike, which have no fractal properties.

The purposes of this paper are to determine the electrochemical behaviors of the layer between the single-crystalline nickel electrode and nickel sulfamate from the viewpoint of the dependence of the reaction impedance on the ac modulation frequency, and to present that the crystallization of nickel ions from nickel sulfamate has a possibility of two charge-transfer reactions comprising the slow reaction $Ni^{2+} + e^- \rightarrow Ni^+_{ads}$ and the fast reaction $Ni^+_{ads} + e^- \rightarrow Ni$.

2. Experimental Section

The experimental procedure for the EIS measurement was as follows. Single-crystalline nickels of 10.0 mm in diameter

* Corresponding author.

10.1021/jp021769w CCC: $22.00
Published on Web 10/22/2002

and 1.0 mm in thickness were prepared as working electrodes, which had a high purity of 99.999 wt % and surface orientation (110) determined to an accuracy of 2.0 degrees. The (110) surfaces were polished using 5, 1, and 0.1 μm diamond powder pastes and finally lapped with a solution of 0.05 μm colloidal silica. The rms roughness of the polished surfaces was an average of 1.9 nm, which was determined from the atomic force microscopy (AFM) images. Poly-crystalline nickel sheets 68 mm long, 60 mm wide, and 0.05 mm thick were prepared for counter electrodes and polished using abrasive sheets of #800. The counter electrode area was 52 times as large as the area of the working electrode. Hence, we can ignore the resistance and capacitance in series of the counter electrode in electrolyte comparing with those of the single-crystalline nickel disk.

Those electrodes cleaned by a wet process were located parallel in a still cell containing (M/L): nickel sulfamate, 0.186 or 1.86; nickel chloride, 0.0386; and boric acid, 0.647. The cell was maintained at pH 4 and at a temperature of 300 or 313 K. The amplitude of the alternative current density applied between the electrodes was small in a range of 0.0764 to 0.19 mA/cm^2. A LCR meter connected to a personal computer through a GP-IB bus was prepared for the EIS measurements in the frequency range from 50 mHz to 100 kHz. AFM with a Si_3N_4 cantilever of a tip radius 15 nm was used to determine the fractal behaviors of the polished single-crystalline nickel surfaces.

3. Results and Discussion

3.1. Fractal Dimension of the Polished (110) Nickel Surfaces. Single-crystalline nickel disks with (110) surfaces were prepared in a fashion described in the Experimental Section. We made investigations into fractal properties of the polished single-crystalline nickel surfaces using AFM that generally gives digitized profile heights $h(K,L)$ for an image comprising M×M pixels where K and L are integers in the x and y directions. The discrete Fourier transform[16] of $h(K,L)$ is

$$H(m_f,n_f) = (1/M^2)\sum_{K,L} h(K,L)\exp[-2\pi(m_fK + n_fL)/M] \quad (1)$$

where m_f and n_f are integers within [0, M − 1] and the ranges of K and L are $-M/2 \le K,L \le M/2 - 1$. The power spectrum dependent on the frequency f yields[17,18]

$$|H(m_f,n_f)|^2 \propto f^{-\gamma} \quad (2)$$

The slope γ obtained from a log−log plot of eq 2 gives the fractal dimension D expressed by

$$D = \frac{8-\gamma}{2} \quad (3)$$

A plot of $|H(m_f,n_f)|^2$ vs f in a log-scale is shown in Figure 1, which gives a slope γ of 3.90. The average fractal dimension becomes 2.0. Hence, the effect of surface roughness on the faradic impedance can be ignored.

Figure 2 shows a typical Nyquist diagram of the single-crystalline nickel disk for nickel sulfamate 1.86 M/L at a temperature of 300 K. It can be seen that there exists only one capacitive loop. The experiment has been repeated several times and the results were consistent within experimental uncertainty. We made more EIS measurements for other experimental conditions in order to make sure the absence of inductive loops at a lower concentration of nickel sulfamate and at a higher temperature of electrolyte. Figures 3 and 4 plot Nyquist diagrams

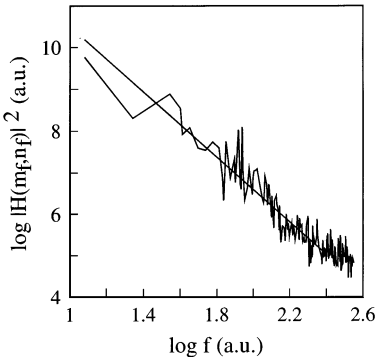

Figure 1. A log-log plot of $|H(m_f, n_f)|^2$ vs f calculated from the AFM image of the polished single-crystalline nickel surface. The solid line gives a value of the exponent γ to calculate the fractal dimension.

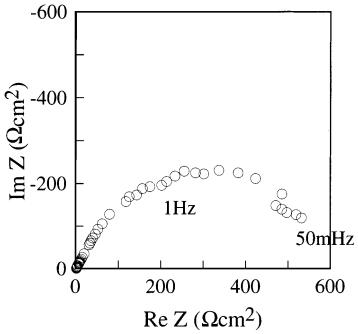

Figure 2. Typical Nyquist diagram for 1.86 M/L nickel sulfamate electrolyte at a temperature of 300 K. Remaining contents are nickel chloride of 3.86 × 10^{-2} M/L and boric acid of 0.647 M/L. The amplitude of the alternative current density is 0.19 mA/cm^2.

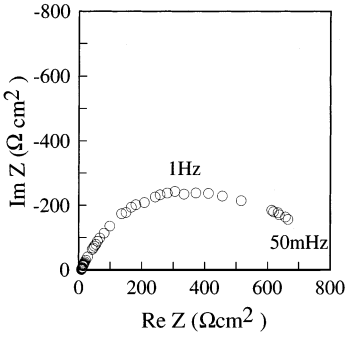

Figure 3. Typical Nyquist diagram for 0.186 M/L nickel sulfamate electrolyte at a temperature of 300 K. Remaining contents are nickel chloride of 3.86 × 10^{-2} M/L and boric acid of 0.647 M/L. The amplitude of the alternative current density is 0.127 mA/cm^2.

for 0.186 M/L nickel sulfamate electrolyte at 300 K and for 1.86 M/L nickel sulfamate electrolyte at 313 K.

3.2. Homogeneous Charge-Transfer Reaction. The reaction impedance for the homogeneous charge-transfer and heterogeneous charge-transfer reactions under a small alternating current density $i = I \sin \omega t$ has been derived by Gerisher.[8,9] Here introducing Gerisher's work briefly, we will show how it leads to a power law that represents the reaction impedance that decreases as a power of the ac modulation frequency. In the case of the homogeneous charge-transfer reaction, the diffusion equation for the homogeneous charge-transfer reaction is

$$\frac{\partial \Delta c}{\partial t} = D\nabla^2 \Delta c - k\Delta c \quad (4)$$

where D is the diffusion coefficient, $\Delta c = c - \bar{c}$, and k is the net rate constant related to the reaction, metal ions (solution)

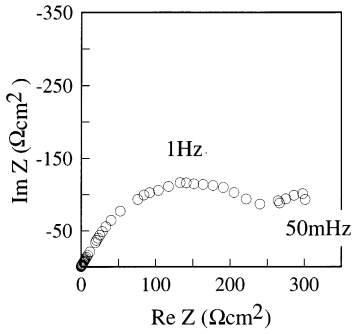

Figure 4. Typical Nyquist diagram for 1.86 M/L nickel sulfamate electrolyte at a temperature of 313 K. Remaining contents are nickel chloride of 3.86×10^{-2} M/L and boric acid of 0.647 M/L. The amplitude of the alternative current density is 0.0764 mA/cm^2.

$\rightarrow$ metal atoms (lattice) (in this study, the two-step reactions $Ni^{2+} + e^- \rightarrow Ni^+_{ads}$ and $Ni^+_{ads} + e^- \rightarrow Ni$ are assumed). Here, Δc is defined by a small change of the ion concentration c from the thermal equilibrium concentration $\bar{c}$, and the change can be small enough to be treated as a perturbation. Eq 4 is solved under the boundary condition

$$\left(\frac{d\Delta c}{dx}\right)_{x=0} = -\frac{\nu I \sin \omega t}{nFD} \tag{5}$$

where n is the charge number, F is the Faraday constant, and ν is the stoichiometric factor. The boundary condition for the homogeneous charge-transfer reaction is given at a plane of $x = 0$ in the x-coordinate normal to the electrode. The plane is located at the outer Helmholtz plane.[19] The solution at $x = 0$ that satisfies eq 5 becomes

$$\Delta c|_{x=0} = \frac{\nu}{nF\sqrt{2D}}\left[\left(\frac{k+\sqrt{k^2+\omega^2}}{k^2+\omega^2}\right)^{1/2} I \sin \omega t - \left(\frac{-k+\sqrt{k^2+\omega^2}}{k^2+\omega^2}\right)^{1/2} I \cos \omega t\right] \tag{6}$$

For $\Delta c/\bar{c} \ll 1$, the overvoltage η is given by

$$\eta = \frac{\nu RT}{nF} \ln \frac{c}{\bar{c}} \cong \frac{\nu RT}{nF} \frac{\Delta c}{\bar{c}} \tag{7}$$

where $c = \bar{c} + \Delta c$. Substituting eq 6 into eq 7, we have

$$\eta = G\left(\sqrt{\frac{k+\sqrt{k^2+\omega^2}}{k^2+\omega^2}} I \sin \omega t - \sqrt{\frac{-k+\sqrt{k^2+\omega^2}}{k^2+\omega^2}} I \cos \omega t\right) \tag{8}$$

where $G = \nu^2 RT/(n^2F^2\bar{c}\sqrt{2D})$.

In an equivalent circuit comprising the reaction resistance Rr and reaction capacitance Cr, the first derivative of the overvoltage $\eta = \mathrm{Rr} I \sin \omega t + \int I \sin \omega t \, dt/\mathrm{Cr}$ with t is

$$\frac{d\eta}{dt} = \mathrm{Rr}\omega I \cos \omega t + \frac{I \sin \omega t}{\mathrm{Cr}} \tag{9}$$

Differentiating eq 8 with respect to t and comparing the result with eq 9, one has

$$\mathrm{Rr} = G\sqrt{\frac{k+\sqrt{\omega^2+k^2}}{\omega^2+k^2}}, \quad (\omega \mathrm{Cr})^{-1} = G\sqrt{\frac{-k+\sqrt{\omega^2+k^2}}{\omega^2+k^2}} \tag{10}$$

In a similar way, the reaction impedance for the heterogeneous charge-transfer reaction[9] is

$$\mathrm{Rr} = H\frac{k}{k^2+\omega^2}, \quad (\omega \mathrm{Cr})^{-1} = H\frac{\omega}{k^2+\omega^2} \tag{11}$$

where $H = \nu^2 RT/n^2F^2\bar{c}$.

In consequence, the reaction impedance obeys the power law,

$$\mathrm{Rr} \propto \omega^{-\alpha}, \quad (\omega \mathrm{Cr})^{-1} \propto \omega^{-\beta} \text{ for } k \ll \omega \tag{12}$$

The exponents α and β are the following: for the homogeneous charge-transfer reaction, $\alpha = 1/2$ and $\beta = 1/2$; for the heterogeneous charge-transfer reaction, $\alpha = 2$ and $\beta = 1$.

A detailed analysis of the charge-transfer reactions in the nickel sulfamate at the single-crystalline nickel electrode is made using the equivalent circuit model shown in Figure 5. The equivalent circuit has the components comprising the electrolyte resistance Re, the double layer capacitance Cd, and the charge-transfer reaction impedance including Rr and Cr. The relationships between these impedances can be easily derived,

$$C1 + \mathrm{Cd} = \frac{(\omega^2 C)^{-1}}{R^2 + (\omega C)^{-2}}, \quad R1 = \frac{R^2 + (\omega C)^{-2}}{R}$$

$$\mathrm{Rr} = \frac{(R1)^{-1}}{(R1)^{-2} + (\omega C1)^2}, \quad (\omega \mathrm{Cr})^{-1} = \frac{\omega C1}{(R1)^{-2} + (\omega C1)^2} \tag{13}$$

Typical plots of Rr vs ω and $(\omega \mathrm{Cr})^{-1}$ vs ω in a log scale are shown in Figure 6 using the data in Figure 2. It can be seen that the reaction resistance and reaction capacitance obey the power law expressed by eq 12. The straight solid lines in Figure 6 best fitted to the data have $\alpha = 0.63$ and $\beta = 0.66$. In a similar way, we have $\alpha = 0.66$ and $\beta = 0.69$ for Figure 3, and $\alpha = 0.60$ and $\beta = 0.64$ for Figure 4. Moreover, eq 13 gives the double layer capacitances Cd, 26.4 μF, 23.5 μF, and 39.2 μF for Figures 2, 3, and 4, respectively. Figure 7 shows that the experimental reaction impedance approximately agrees with theoretical values for the homogeneous charge-transfer reaction. We assume $G = 450$ (Ω s$^{-1/2}$) and $k = 1.2$ (s^{-1}) in Figure 7. Hence, taking into consideration the theoretical exponents of $\alpha = \beta = 1/2$ for the homogeneous charge-transfer reaction, we may conclude that the charge-transfer reaction in the nickel sulfamate electrolyte is rather homogeneous than heterogeneous.

3.3. Absence of Inductive Loops. In this study, the experiments have been repeated several times, but the diagrams show only one capacitive loop and the absence of inductive loops, which are different from the EIS results in Watt's electrolyte[1,2] containing $NiSO_4$, $NiCl_2$, and H_3BO_3. The amplitudes of the ac current density in Figures 2−4 were small enough to apply theoretical treats.

Here, let us consider a condition for the presence of one inductive loop in two successive faradic reaction steps. As stated in the homogeneous charge-transfer reaction, the reaction impedances have no inductive element. Therefore, for simplicity we ignore the diffusion process and derive a condition that one inductive loop appears in the Nyquist diagram for two successive faradic reaction steps using a linear perturbation theory and equivalent circuit model. Here, only electrochemical impedance without diffusion is discussed. A small alternative current

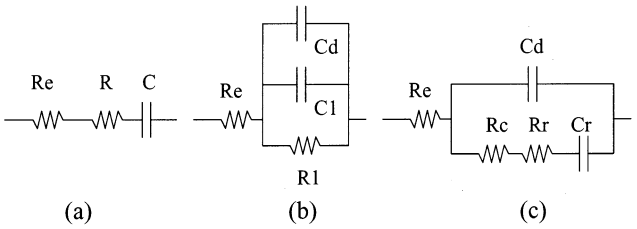

Figure 5. Equivalent circuit to calculate the reaction impedance including Rr and Cr. (a) Resistance Re + *R* and capacitance *C* in series measured by a LCR meter. Re is a resistor due to nickel sulfamate electrolyte. (b) Impedance in parallel, here Cd denotes the capacitance of the double layer. (c) Equivalent circuit for the calculations of Rr and Cr in this study.

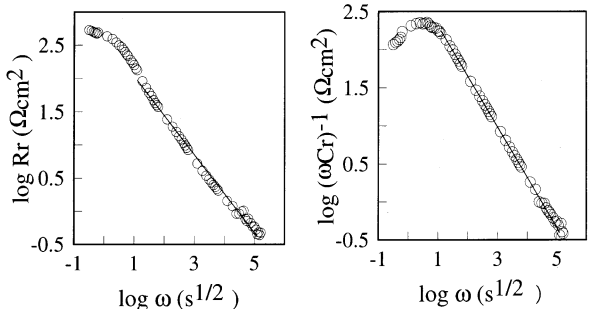

Figure 6. Typical plots of Rr vs ω and $(\omega\mathrm{Cr})^{-1}$ vs ω in a log scale using the data in Figure 2. The straight solid lines best fitted to the data give $\alpha = 0.63$ and $\beta = 0.66$.

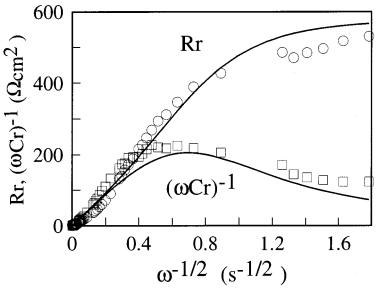

Figure 7. Dependence of Rr and $(\omega\mathrm{Cr})^{-1}$ on ω. The solid line *s* indicate the theoretical values based on the homogeneous charge-transfer model in the case of $G = 450$ ($\Omega\ s^{-1/2}$) and $k = 1.2$ (s^{-1}).

applied between working and counter electrodes causes an overvoltage required for electrochemical reactions. The crystallization of nickel ions in nickel sulfamate takes place in two successive faradic reactions of adsorbed nickel ions[2,12] such as

$$\mathrm{Ni}^{2+} + \mathrm{e}^- \rightarrow \mathrm{Ni}^+_{\mathrm{ads}} \tag{14}$$

$$\mathrm{Ni}^+_{\mathrm{ads}} + \mathrm{e}^- \rightarrow \mathrm{Ni} \tag{15}$$

Let the rate of formation of $\mathrm{Ni}^+_{\mathrm{ads}}$ be v_1 and the rate of formation of nickel atoms be v_2. For a small alternative current $\Delta i = I \exp(j\omega t)$ where t is time, v_1 and v_2 can be expanded in linear series,

$$\Delta v_i = v_i - v_i^0 = \left(\frac{\partial v_i}{\partial \Delta c}\right)\Delta c + \left(\frac{\partial v_i}{\partial \Delta \eta}\right)\Delta \eta, \quad (i = 1, 2) \tag{16}$$

where Δc denotes a changes of the concentration $\mathrm{Ni}^+_{\mathrm{ads}}$ from the steady-state concentration $\bar{c}$, $\Delta\eta$ denotes a changes of the overvoltage from the steady-state overvoltage η_o, and v_1^0 and v_2^0 denote the rate in the steady state. Equation 14 should satisfy the continuity equations,

$$\frac{\mathrm{d}\Delta c}{\mathrm{d}t} = \Delta v_1 - \Delta v_2 \tag{17}$$

$$\Delta i = F(\Delta v_1 + \Delta v_2) \tag{18}$$

It is clear that for the steady-state condition, $v_1^0 = v_2^0 = v_0$. According to Gerischer[8,9] and Matlosz,[20] the rates v_1 and v_2 are expressed as

$$v_i = k_i c \exp(b_i \eta), \quad (i = 1, 2) \tag{19}$$

where b_i is a constant and k_i is the rate constant. Equation 19 leads to

$$\frac{\partial v_i}{\partial \Delta c} = k_i \exp(b_i \eta_0), \quad \frac{\partial v_i}{\partial \Delta \eta} = b_i v_0 \exp(b_i \Delta \eta) \quad (i = 1, 2) \tag{20}$$

Substituting eqs 16 and 20 into eq 17, we have for a small $|\Delta\eta|$

$$\Delta c = \frac{(b_1 - b_2)v_0}{j\omega - k_1 \exp(b_1\eta_0) + k_2 \exp(b_2\eta_0)}\Delta\eta \tag{21}$$

Here $\mathrm{d}\Delta c/\mathrm{d}t = j\omega\Delta c$ is used. In a similar way, eq 18 can be rewritten as

$$I = [k_1 \exp(b_1\eta_0) + k_2 \exp(b_2\eta_0)]\Delta c + (b_1 + b_2)v_0\Delta\eta \tag{22}$$

Hence, eqs 21 and 22 give the faradaic admittance Y,

$$Y = (b_1 + b_2)v_0 + \frac{\tau v_0[k_1 \exp(b_1\eta_0) + k_2 \exp(b_2\eta_0)](b_2 - b_1)}{1 + \omega^2\tau^2} - j\frac{\omega\tau^2 v_0[k_1 \exp(b_1\eta_0) + k_2 \exp(b_2\eta_0)](b_2 - b_1)}{1 + \omega^2\tau^2} \tag{23}$$

where $\tau^{-1} = -k_1 \exp(b_1\eta_0) + k_2 \exp(b_2\eta_0)$. The third term on the right-hand side in eq 23 represents an inductive element when it has a positive sign, i.e., $b_2 > b_1$. From $v_1^0 = v_2^0 = v_0$, the condition $b_2 > b_1$ is equivalent to

$$k_1 > k_2 \tag{24}$$

This indicates that reaction 14 is a fast-step reaction and the reaction 15 is a slow-step reaction, and only emphasizes that an accumulation of adsorbed nickel ions is needed to observe as an inductive element in faradaic impedance measurements. In other words, for $k_1 < k_2$, the reaction appears to take place in one reaction step even if in two successive reaction steps. The charge-transfer rate is thought to be $k_1 < k_2$ according to eq 24 because no inductive loops are observed. The crystallization of nickel ions in the sulfamate nickel electrolyte may occur in the slow reaction $\mathrm{Ni}^{2+} + \mathrm{e}^- \rightarrow \mathrm{Ni}^+_{\mathrm{ads}}$ and in the fast reaction $\mathrm{Ni}^+_{\mathrm{ads}} + \mathrm{e}^- \rightarrow \mathrm{Ni}$.

4. Conclusion

Electrochemical impedance spectroscopy was used to make investigations into electrochemical reactions on (110) single-crystalline nickel surfaces in nickel sulfamate electrolyte. The EIS measurements show the absence of inductive loops in their Nyquist diagrams ranging from 50 mHz to 100 kHz, which suggests that the electrocrystallization of Ni^{2+} ions will take place in the slow reaction $\mathrm{Ni}^{2+} + \mathrm{e}^- \rightarrow \mathrm{Ni}^+_{\mathrm{abs}}$ and in the fast

reaction $Ni^{+}_{abs} + e^{-} \rightarrow Ni$. Moreover, the impedance results are discussed in view of the reaction impedance dependent on the ac modulation frequency and compared with the theoretical values predicted by the reaction impedance model. It is found that the reaction impedance obeys the power law and the charge-transfer reaction is homogeneous.

Acknowledgment. This work was supported by Grant-in-Aid for Scientific Research (C), No. 13650029 by the Ministry of Education, Science, and Culture of Japan.

References and Notes

(1) Chang, C.-C.; West, A. C. *J. Electrochem. Soc.* **1997**, *144*, 3050.
(2) Holm, M.; O'keefe, T. J. *J. Appl. Electrochem.* **2000**, *30*, 1125.
(3) Bischofberger, R.; Zimmermann, H.; Staufert, G. *Sensors Acutuators A* **1997**, *61*, 392.
(4) O'M Bockris, J.; Reddy, A. K. N.; G-Aldeco, M. *Modern Electrochemistry 2A*; Kluwer Academic: New York, 2000; pp 9−13.
(5) Warburg, E. *Annu. Phys. Chem.* **1899**, *67*, 493.
(6) Ramos-Barrado, J. R.; Montenegro, P. G.; Cambón, C. C. *J. Chem. Phys.* **1996**, *105*, 2813.
(7) Vetter, K. J. *Electrochemical Kinetics*; Academic Press: New York, 1967; pp 253−263.
(8) Gerischer, H. *Z. Phys. Chem.* **1951**, *198*, 286.
(9) Gerischer, H. *Z. Phys. Chem.* **1952**, *201*, 55.
(10) Liu, X. Y. *J. Chem. Phys.* **1999**, *111*, 1628.
(11) Asanuma, M.; Aoyagi, R. *J. Chem. Phys.* **1997**, *106*, 9944.
(12) Lachenwitzer, A.; Magnussen, O. M. *J. Phys. Chem. B* **2000**, *104*, 7414.
(13) Armstrong, R. D.; Henderson, M. *J. Electroanal. Chem.* **1972**, *39*, 81.
(14) Larsen A. E.; Grier, D. G.; *Phy. Rev. E* **1995**, *52*, R2161.
(15) Bisquert, J. *Phys. Chem. Chem. Phys.* **2000**, *2*, 4185.
(16) Saitou, M.; Hokama, M.; Oshikawa, W. *Appl. Surf. Sci.* **2001**, *185*, 79.
(17) Dumas, Ph.; Bouffakhreddine, B.; Amra, C.; Vatel, O.; Andre, E.; Galindo, R.; Salvan, F. *Europhys.* **1993**, *22*, 717.
(18) Oliva, A. I.; Anguiano, E.; Sacedó, J. L.; Aguilar, M.; Méndez, J. A.; Aznárez, J. A. *Phys. Rev. B* **1999**, *60*, 2720.
(19) Pandey, P. K.; Sahu, S. N.; Chandra, S. *Handbook of Semiconductor Electrodeposition*; Marcel Dekker Inc.: New York, 1996.
(20) Matlosz, M. *J. Electrochem. Soc.* **1993**, *140*, 2272.